



Observation of the decay $\Lambda_b^0 \rightarrow pK^- \mu^+ \mu^-$ and a search for CP violation

The LHCb collaboration[†]

Abstract

A search for CP violation in the decay $\Lambda_b^0 \rightarrow pK^- \mu^+ \mu^-$ is presented. This decay is mediated by flavour-changing neutral-current transitions in the Standard Model and is potentially sensitive to new sources of CP violation. The study is based on a data sample of proton-proton collisions recorded with the LHCb experiment, corresponding to an integrated luminosity of 3 fb^{-1} . The $\Lambda_b^0 \rightarrow pK^- \mu^+ \mu^-$ decay is observed for the first time, and two observables that are sensitive to different manifestations of CP violation are measured, $\Delta\mathcal{A}_{CP} \equiv \mathcal{A}_{CP}(\Lambda_b^0 \rightarrow pK^- \mu^+ \mu^-) - \mathcal{A}_{CP}(\Lambda_b^0 \rightarrow pK^- J/\psi)$ and $a_{CP}^{\hat{T}\text{-odd}}$, where the latter is based on asymmetries in the angle between the $\mu^+ \mu^-$ and pK^- decay planes. These are measured to be

$$\begin{aligned}\Delta\mathcal{A}_{CP} &= (-3.5 \pm 5.0 \text{ (stat)} \pm 0.2 \text{ (syst)}) \times 10^{-2}, \\ a_{CP}^{\hat{T}\text{-odd}} &= (1.2 \pm 5.0 \text{ (stat)} \pm 0.7 \text{ (syst)}) \times 10^{-2},\end{aligned}$$

and no evidence for CP violation is found.

Published in JHEP 06 (2017) 108

© CERN on behalf of the LHCb collaboration, licence CC-BY-4.0.

[†]Authors are listed at the end of this paper.

1 Introduction

The phenomenon of CP violation (CPV), related to the difference in behaviour between matter and antimatter, remains an intriguing topic more than fifty years after its discovery in the neutral kaon system [1]. Within the Standard Model of particle physics (SM), CPV is incorporated by a single, irreducible weak phase in the Cabibbo-Kobayashi-Maskawa (CKM) quark mixing matrix [2,3]. However, the amount of CPV in the SM is insufficient to explain the observed level of matter-antimatter asymmetry in the Universe [4–6]. Therefore, new sources of CPV beyond the SM are expected to exist. Experimental observations of CPV remain confined to the B - and K -meson systems. Recently, the first evidence for CPV in $\Lambda_b^0 \rightarrow p\pi^-\pi^+\pi^-$ was found at the level of 3.3 standard deviations [7] and a systematic study of CPV in beauty baryon decays has now begun.

Among dedicated heavy-flavour physics experiments, the LHCb detector [8] is unique in having access to a wide range of decay modes of numerous b -hadron species. Beauty baryons are produced copiously at the LHC, and within the LHCb detector acceptance the production ratio of $B^0 : \Lambda_b^0 : B_s^0$ particles is approximately 4 : 2 : 1 [9]. The LHCb collaboration has previously searched for CPV in $\Lambda_b^0 \rightarrow p\pi^-J/\psi$ and $\Lambda_b^0 \rightarrow pK^-J/\psi$ decays [10], as well as in charmless $\Lambda_b^0 \rightarrow pK_s^0\pi^-$, $\Lambda_b^0 \rightarrow \Lambda\phi$ and $\Lambda_b^0 \rightarrow \Lambda h^+h^-$ transitions [11–13].

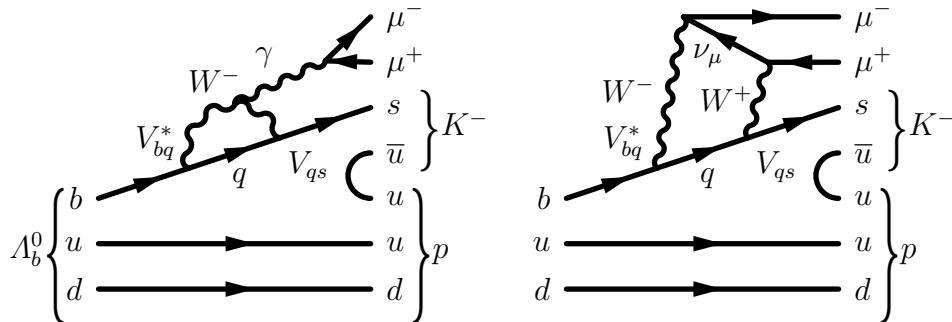


Figure 1: Diagrams for the decay $\Lambda_b^0 \rightarrow pK^-\mu^+\mu^-$, in which V_{bq} and V_{qs} are CKM matrix elements and q represents one of the three up-type quarks u, c or t , the t -quark contribution being dominant. The $u\bar{u}$ pairs originate from the hadronization process.

In this paper, a search for CPV in the hitherto unobserved decay $\Lambda_b^0 \rightarrow pK^-\mu^+\mu^-$ is reported.¹ It is a flavour-changing neutral-current process with the underlying quark-level transition $b \rightarrow s\mu^+\mu^-$. The leading-order transition amplitudes in the SM are described by the loop diagrams shown in Fig. 1. In extensions to the SM, new heavy particles could contribute to the amplitudes with additional weak phases, providing new sources of CPV [14,15]. The limited amount of CPV predicted for the decay $\Lambda_b^0 \rightarrow pK^-\mu^+\mu^-$ in the SM [15,16], following from the CKM matrix elements shown in Fig. 1, makes this decay particularly sensitive to CPV effects from physics beyond the SM.

¹The inclusion of charge-conjugate processes is implied throughout this paper, unless stated otherwise.

2 CP -odd observables

Two types of CP -odd observables are studied in this paper. Following Refs. [7, 17], the differential rate of any pair of CP -conjugate processes can be decomposed into four parts with definite even and odd transformation properties under the CP and motion-reversal \widehat{T} operators. Here, \widehat{T} is the unitary operator that reverses both momentum and spin three-vectors, to be distinguished from the antiunitary time-reversal operator T which reverses initial and final states.

A \widehat{T} -even and CP -odd asymmetry, \mathcal{A}_{CP} , is related to the raw asymmetry \mathcal{A}_{raw} of the observed decay candidates

$$\mathcal{A}_{\text{raw}} \equiv \frac{N(\Lambda_b^0 \rightarrow pK^- \mu^+ \mu^-) - N(\bar{\Lambda}_b^0 \rightarrow \bar{p}K^+ \mu^- \mu^+)}{N(\Lambda_b^0 \rightarrow pK^- \mu^+ \mu^-) + N(\bar{\Lambda}_b^0 \rightarrow \bar{p}K^+ \mu^- \mu^+)}, \quad (1)$$

via

$$\mathcal{A}_{\text{raw}} \approx \mathcal{A}_{CP}(\Lambda_b^0 \rightarrow pK^- \mu^+ \mu^-) + \mathcal{A}_{\text{prod}}(\Lambda_b^0) - \mathcal{A}_{\text{reco}}(K^+) + \mathcal{A}_{\text{reco}}(p), \quad (2)$$

where $\mathcal{A}_{\text{prod}}(\Lambda_b^0)$ is the Λ_b^0 production asymmetry, due to the pp initial state, and $\mathcal{A}_{\text{reco}}(K^+)$ and $\mathcal{A}_{\text{reco}}(p)$ are the reconstruction asymmetries for kaons and protons, mainly due to the different interaction cross-sections of particles and antiparticles with the detector material. By measuring the difference of raw asymmetries between the signal and the Cabibbo-favoured control mode $\Lambda_b^0 \rightarrow pK^- J/\psi (\rightarrow \mu^+ \mu^-)$, the production and reconstruction asymmetries cancel to a good approximation. No significant CPV is expected in the latter decay, since its amplitude is dominated by tree-level CP -conserving diagrams, which leads to

$$\begin{aligned} \Delta \mathcal{A}_{CP} &\equiv \mathcal{A}_{CP}(\Lambda_b^0 \rightarrow pK^- \mu^+ \mu^-) - \mathcal{A}_{CP}(\Lambda_b^0 \rightarrow pK^- J/\psi) \\ &\approx \mathcal{A}_{\text{raw}}(\Lambda_b^0 \rightarrow pK^- \mu^+ \mu^-) - \mathcal{A}_{\text{raw}}(\Lambda_b^0 \rightarrow pK^- J/\psi). \end{aligned} \quad (3)$$

Imperfect cancellation in the production and reconstruction asymmetries can arise from differences in the kinematic distributions of the signal and control modes. A weighting procedure, discussed in Sec. 5, is applied to correct for this, with residual effects considered as a source of systematic uncertainty in Sec. 6.

A pair of \widehat{T} -odd and P -odd observables, $A_{\widehat{T}}$ and $\bar{A}_{\widehat{T}}$, is obtained by defining the \widehat{T} -odd triple products of the final-state particle momenta in the Λ_b^0 rest frame

$$C_{\widehat{T}} \equiv \vec{p}_{\mu^+} \cdot (\vec{p}_p \times \vec{p}_{K^-}), \quad (4)$$

$$\bar{C}_{\widehat{T}} \equiv \vec{p}_{\mu^-} \cdot (\vec{p}_{\bar{p}} \times \vec{p}_{K^+}), \quad (5)$$

and taking the asymmetries

$$A_{\widehat{T}} \equiv \frac{N(C_{\widehat{T}} > 0) - N(C_{\widehat{T}} < 0)}{N(C_{\widehat{T}} > 0) + N(C_{\widehat{T}} < 0)}, \quad \bar{A}_{\widehat{T}} \equiv \frac{\bar{N}(-\bar{C}_{\widehat{T}} > 0) - \bar{N}(-\bar{C}_{\widehat{T}} < 0)}{\bar{N}(-\bar{C}_{\widehat{T}} > 0) + \bar{N}(-\bar{C}_{\widehat{T}} < 0)}, \quad (6)$$

where $N(\bar{N})$ is the number of Λ_b^0 ($\bar{\Lambda}_b^0$) signal candidates. These asymmetries are measured from the angular distributions of the decay products, with $C_{\widehat{T}}$ being proportional to $\sin \chi$ [18], where χ is the angle between the decay planes of the $\mu^+ \mu^-$ and pK^- systems in the Λ_b^0 rest frame, as shown in Fig. 2.

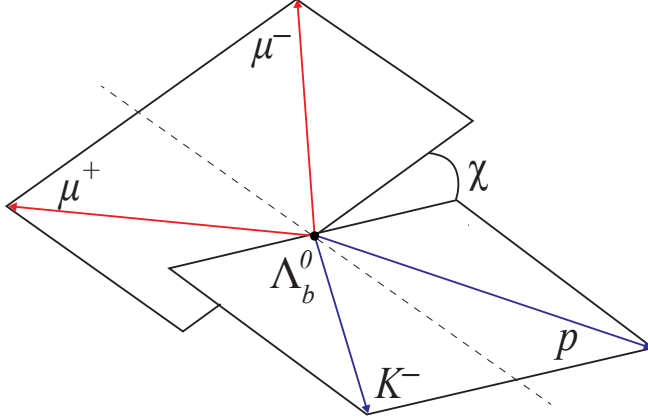


Figure 2: Definition of the angle χ for $\Lambda_b^0 \rightarrow p K^- \mu^+ \mu^-$ decays, in the Λ_b^0 rest frame.

The observables $A_{\hat{T}}$ and $\bar{A}_{\hat{T}}$ are P - and \hat{T} -odd but are not sensitive to CPV effects [17]. Following Ref. [18], CP -odd and P -odd observables are defined as

$$a_{CP}^{\hat{T}\text{-odd}} \equiv \frac{1}{2} (A_{\hat{T}} - \bar{A}_{\hat{T}}), \quad a_P^{\hat{T}\text{-odd}} \equiv \frac{1}{2} (A_{\hat{T}} + \bar{A}_{\hat{T}}), \quad (7)$$

where a non-zero value of $a_{CP}^{\hat{T}\text{-odd}}$ or $a_P^{\hat{T}\text{-odd}}$ would signal CP or parity violation, respectively. These observables are by construction largely insensitive to the Λ_b^0 production asymmetry and detector-induced charge asymmetries.

The observables $\Delta\mathcal{A}_{CP}$ and $a_{CP}^{\hat{T}\text{-odd}}$ are sensitive to different manifestations of CPV [17]. The CP asymmetry \mathcal{A}_{CP} depends on the interference of \hat{T} -even amplitudes, which can be written as $\mathcal{M}_i^e = a_i^e \exp[i(\delta_i^e + \phi_i^e)]$, where δ_i^e are CP -even strong phases, $CP(\delta_i^e) = \delta_i^e$, and ϕ_i^e are CP -odd weak phases, $CP(\phi_i^e) = -\phi_i^e$. This convention is such that all CPV effects are encoded in the CP -odd weak phases. The \hat{T} -even and CP -odd part of the differential rate turns out to be

$$\frac{d\Gamma}{d\Phi} \Big|_{CP\text{-odd}}^{\hat{T}\text{-even}} \propto a_1^e a_2^e \sin(\delta_1^e - \delta_2^e) \sin(\phi_1^e - \phi_2^e), \quad (8)$$

where only two \hat{T} -even amplitudes are considered for simplicity. Therefore, \mathcal{A}_{CP} is enhanced when the strong phase difference between the two amplitudes is large.

On the other hand, $a_{CP}^{\hat{T}\text{-odd}}$ depends on the interference between \hat{T} -even and \hat{T} -odd amplitudes, the latter written as $\mathcal{M}_i^o = a_i^o \exp[i(\delta_i^o + \phi_i^o + \pi/2)]$, following the same convention used for \hat{T} -even amplitudes. The \hat{T} -odd and CP -odd part of the differential rate is therefore

$$\frac{d\Gamma}{d\Phi} \Big|_{CP\text{-odd}}^{\hat{T}\text{-odd}} \propto a_1^e a_1^o \sin(\delta_1^e - \delta_1^o) \sin(\phi_1^e - \phi_1^o), \quad (9)$$

where one \hat{T} -even and one \hat{T} -odd amplitudes are considered for simplicity. As a consequence, $a_{CP}^{\hat{T}\text{-odd}}$ is enhanced when the strong phase difference vanishes. Furthermore, the observables $\Delta\mathcal{A}_{CP}$ and $a_{CP}^{\hat{T}\text{-odd}}$ are sensitive to different types of CPV effects from physics beyond the SM [16].

3 Detector and simulation

The LHCb detector [8,19] is a single-arm forward spectrometer covering the pseudorapidity range $2 < \eta < 5$, designed for the study of particles containing b or c quarks. The detector includes a high-precision tracking system consisting of a silicon-strip vertex detector surrounding the pp interaction region, a large-area silicon-strip detector located upstream of a dipole magnet with a bending power of about 4 Tm, and three stations of silicon-strip detectors and straw drift tubes placed downstream of the magnet. The tracking system provides a measurement of momentum, p , of charged particles with a relative uncertainty that varies from 0.5% at low momentum to 1.0% at 200 GeV/ c . The minimum distance of a track to a primary vertex (PV), the impact parameter (IP), is measured with a resolution of $(15 + 29/p_T) \mu\text{m}$, where p_T is the component of the momentum transverse to the beam, in GeV/ c . Different types of charged hadrons are distinguished using information from two ring-imaging Cherenkov detectors. Photons, electrons and hadrons are identified by a calorimeter system consisting of scintillating-pad and preshower detectors, an electromagnetic calorimeter and a hadronic calorimeter. Muons are identified by a system composed of alternating layers of iron and multiwire proportional chambers. The online event selection is performed by a trigger [20], which consists of a hardware stage, based on information from the calorimeter and muon systems, followed by a software stage, which applies a full event reconstruction.

Simulated signal events are used to determine the effect of the detector geometry, trigger, reconstruction and selection on the angular distributions of the signal and $\Lambda_b^0 \rightarrow pK^- J/\psi$ control sample. Additional simulated samples are used to estimate the contribution from specific background processes. In the simulation, pp collisions are generated using PYTHIA [21,22] with a specific LHCb configuration [23]. Decays of hadronic particles are described by EVTGEN [24], in which final-state radiation is generated using PHOTOS [25]. The interaction of the generated particles with the detector, and its response, are implemented using the GEANT4 toolkit [26], as described in Ref. [27].

4 Selection of signal candidates

The present analysis is performed using proton-proton collision data corresponding to 1 and 2 fb $^{-1}$ of integrated luminosity, collected with the LHCb detector in 2011 and 2012, at centre-of-mass energies of 7 and 8 TeV, respectively. The $\Lambda_b^0 \rightarrow pK^- \mu^+ \mu^-$ candidates are reconstructed from a proton, a kaon and two muon candidates originating from a common vertex, and are selected using information from the particle identification system. The Λ_b^0 flavour is determined from the charge of the kaon candidate, *i.e.* Λ_b^0 for negative and $\bar{\Lambda}_b^0$ for positive kaons. Only candidates with reconstructed invariant mass, $m(pK^- \mu^+ \mu^-)$, in the range [5350, 6000] MeV/ c^2 and a pK^- invariant mass, $m(pK^-)$, below 2350 MeV/ c^2 are retained, with the latter requirement being applied to reduce the combinatorial background contribution. The spectrum in the dimuon mass squared, q^2 , is considered, excluding the resonance regions $q^2 \in [0.98, 1.10]$, [8.0, 11.0] and [12.5, 15.0] GeV $^2/c^4$ that correspond to the masses of the $\phi(1020)$, J/ψ , and $\psi(2S)$ mesons, respectively.

Several background contributions from exclusive decays are identified and rejected. These are $B_s^0 \rightarrow K^+ K^- \mu^- \mu^+$ and $\bar{B}^0 \rightarrow K^- \pi^+ \mu^+ \mu^-$ decays, in which a kaon or a pion is misidentified as a proton, and $\Lambda_b^0 \rightarrow pK^- \mu^+ \mu^-$ decays, in which proton and

kaon assignments are interchanged. Background also arises from $\Lambda_b^0 \rightarrow pK^- J/\psi$ and $\Lambda_b^0 \rightarrow pK^- \psi(2S)$ decays in which a muon is misidentified as a kaon and the kaon as a muon. These components are effectively eliminated by tightened particle identification requirements combined with selection criteria on invariant masses calculated under the appropriate mass hypothesis (*e.g.* assigning the kaon mass to the candidate proton to identify possible $B_s^0 \rightarrow K^+ K^- \mu^- \mu^+$ background decays). After these requirements the background contribution from the above decays is negligible. No indication of other specific background decays is observed. The remaining combinatorial background is suppressed by means of a boosted decision tree (BDT) classifier [28, 29] with an adaptive boosting algorithm [30]. The BDT is constructed from variables that discriminate between signal and background, based on their kinematic, topological and particle identification properties, as well as the isolation of the final-state tracks [31, 32]. Simulated $\Lambda_b^0 \rightarrow pK^- \mu^+ \mu^-$ events in which the decay products are uniformly distributed in phase space are used as the signal training sample and a correction for known differences between data and simulation is applied. Candidates from data in the high mass region, $m(pK^- \mu^+ \mu^-) > 5800 \text{ MeV}/c^2$, are used as the background training sample and then removed from the window of the mass fit described below. After optimisation of the significance, $S/\sqrt{S+B}$, where S and B are the number of signal and background candidates in the region $m(pK^- \mu^+ \mu^-) \in [5400, 5800] \text{ MeV}/c^2$, the BDT classifier retains only 0.14% of the combinatorial background candidates, with a signal efficiency of 51%. Events in which more than one Λ_b^0 candidate survives the selection constitute less than 1% of the sample and all candidates are retained; the systematic uncertainty associated with this is negligible. The identical selection is applied to the control-mode $\Lambda_b^0 \rightarrow pK^- J/\psi$, except that the dimuon squared mass is required to be in the range $[9.0, 10.5] \text{ GeV}^2/c^4$.

5 Asymmetry measurements

For the $\Delta\mathcal{A}_{CP}$ measurement, the data are divided into two subsamples according to the Λ_b^0 flavour. For the measurements of the triple-product asymmetries, four subsamples are defined by the combination of the Λ_b^0 flavour and the sign of $C_{\hat{T}}$ (or $\bar{C}_{\hat{T}}$ for $\bar{\Lambda}_b^0$). The reconstruction efficiencies are studied with simulated events and are found to be equal for all subsamples.

The observable $\Delta\mathcal{A}_{CP}$ can be sensitive to kinematic differences between the signal and control-mode decays that affect the cancellation of the detection asymmetries in Eq. 3. This is taken into account by assigning a weight to each $\Lambda_b^0 \rightarrow pK^- J/\psi$ candidate such that the resulting proton and kaon momentum distributions match those of the signal $\Lambda_b^0 \rightarrow pK^- \mu^+ \mu^-$ decays. These weights are determined from simulation samples for the signal and control modes. No such weighting is required for $a_{CP}^{\hat{T}\text{-odd}}$ and $a_{\bar{P}}^{\hat{T}\text{-odd}}$, since these observables involve only one decay mode.

The asymmetry \mathcal{A}_{raw} is determined from a simultaneous extended maximum likelihood unbinned fit to the Λ_b^0 and $\bar{\Lambda}_b^0$ invariant mass distributions. The $A_{\hat{T}}$ and $\bar{A}_{\hat{T}}$ asymmetries are determined by means of a simultaneous extended maximum likelihood unbinned fit to the four subsamples defined above. The signal model for all fits is the sum of two Crystal Ball functions [33], one with a low-mass power-law tail and one with a high-mass tail, and a Gaussian function, all sharing the same peak position. Only the peak position, the total width of the composite function and the overall normalization are free to vary, with all

other shape parameters fixed from a fit to simulated decays. The background is modelled by an exponential function. The raw asymmetry \mathcal{A}_{raw} is incorporated in the fit model as

$$N_{\Lambda_b^0} = N_{\Lambda_b^0} \frac{1 - \mathcal{A}_{\text{raw}}}{1 + \mathcal{A}_{\text{raw}}}, \quad (10)$$

and $\Delta\mathcal{A}_{CP}$ is derived from the raw asymmetries measured in the signal and control modes according to Eq. 3. The asymmetries $A_{\hat{T}}$ and $\bar{A}_{\hat{T}}$ are included in the fit as

$$\begin{aligned} N_{\Lambda_b^0, C_{\hat{T}} > 0} &= \frac{1}{2} N_{\Lambda_b^0} (1 + A_{\hat{T}}), & N_{\Lambda_b^0, C_{\hat{T}} < 0} &= \frac{1}{2} N_{\Lambda_b^0} (1 - A_{\hat{T}}), \\ N_{\bar{\Lambda}_b^0, -\bar{C}_{\hat{T}} > 0} &= \frac{1}{2} N_{\bar{\Lambda}_b^0} (1 + \bar{A}_{\hat{T}}), & N_{\bar{\Lambda}_b^0, -\bar{C}_{\hat{T}} < 0} &= \frac{1}{2} N_{\bar{\Lambda}_b^0} (1 - \bar{A}_{\hat{T}}), \end{aligned} \quad (11)$$

and the observables $a_{CP}^{\hat{T}\text{-odd}}$ and $a_P^{\hat{T}\text{-odd}}$ are computed from $A_{\hat{T}}$ and $\bar{A}_{\hat{T}}$, which are found to be uncorrelated. Background yields are fitted independently for each subsample, while all the signal shape parameters are shared among the subsamples.

The invariant mass distributions of $\Lambda_b^0 \rightarrow pK^- \mu^+ \mu^-$ and $\Lambda_b^0 \rightarrow pK^- J/\psi$ candidates, with fit results superimposed, are shown in Fig. 3. The \mathcal{A}_{raw} asymmetries are found to be $(-2.8 \pm 5.0) \times 10^{-2}$ for signal decays and $(2.0 \pm 0.7) \times 10^{-2}$ for the control mode, which yields efficiency-uncorrected $\Delta\mathcal{A}_{CP} = (-4.8 \pm 5.0) \times 10^{-2}$. The total signal yields from the fits to the data are 600 ± 44 candidates for $\Lambda_b^0 \rightarrow pK^- \mu^+ \mu^-$, and $22\,911 \pm 230$ for $\Lambda_b^0 \rightarrow pK^- J/\psi$ decays. The uncertainties are statistical only. This represents the first observation of the $\Lambda_b^0 \rightarrow pK^- \mu^+ \mu^-$ decay mode.

The invariant mass distributions of the $\Lambda_b^0 \rightarrow pK^- \mu^+ \mu^-$ subsamples used for the $A_{\hat{T}}$ and $\bar{A}_{\hat{T}}$ measurements, with fit results superimposed, are shown in Fig. 4. From the signal yields, the triple-product asymmetries are found to be $A_{\hat{T}} = (-2.8 \pm 7.2) \times 10^{-2}$ and $\bar{A}_{\hat{T}} = (4.0 \pm 6.9) \times 10^{-2}$, and the resulting efficiency-uncorrected parity- and CP -violating observables are $a_P^{\hat{T}\text{-odd}} = (-3.4 \pm 5.0) \times 10^{-2}$ and $a_{CP}^{\hat{T}\text{-odd}} = (0.6 \pm 5.0) \times 10^{-2}$, where again the uncertainties are statistical only.

6 Systematic uncertainties

The analysis method depends upon the weighting procedure discussed in Sec. 5 to equalise the kinematic distributions of the protons and kaons between the signal and control modes. For $\Delta\mathcal{A}_{CP}$, the associated systematic uncertainty is estimated by varying the weights within their uncertainties and taking the largest deviation, $\pm 0.15 \times 10^{-2}$, as a systematic uncertainty. No weighting is needed for $a_{CP}^{\hat{T}\text{-odd}}$ and $a_P^{\hat{T}\text{-odd}}$, and therefore no systematic uncertainty is assigned. Instead, the effects of selection and detector acceptance on the triple-product asymmetries are estimated by measuring $a_{CP}^{\hat{T}\text{-odd}}(pK^- J/\psi)$ on the control mode, $\Lambda_b^0 \rightarrow pK^- J/\psi$. A value of $(0.5 \pm 0.7) \times 10^{-2}$ is obtained. For this mode negligible CPV is expected, and the statistical uncertainty of the measured asymmetry is assigned as the corresponding systematic uncertainty on the observables $a_{CP}^{\hat{T}\text{-odd}}$ and $a_P^{\hat{T}\text{-odd}}$. The effects of the reconstruction efficiency on the measured observables are considered by weighting each event by the inverse of the efficiency extracted from simulated events. This leads to a change in the central values of $+1.3 \times 10^{-2}$ on $\Delta\mathcal{A}_{CP}$, of $+0.6 \times 10^{-2}$ on $a_{CP}^{\hat{T}\text{-odd}}$ and of -1.4×10^{-2} on $a_P^{\hat{T}\text{-odd}}$. A systematic uncertainty is assigned by varying the efficiencies

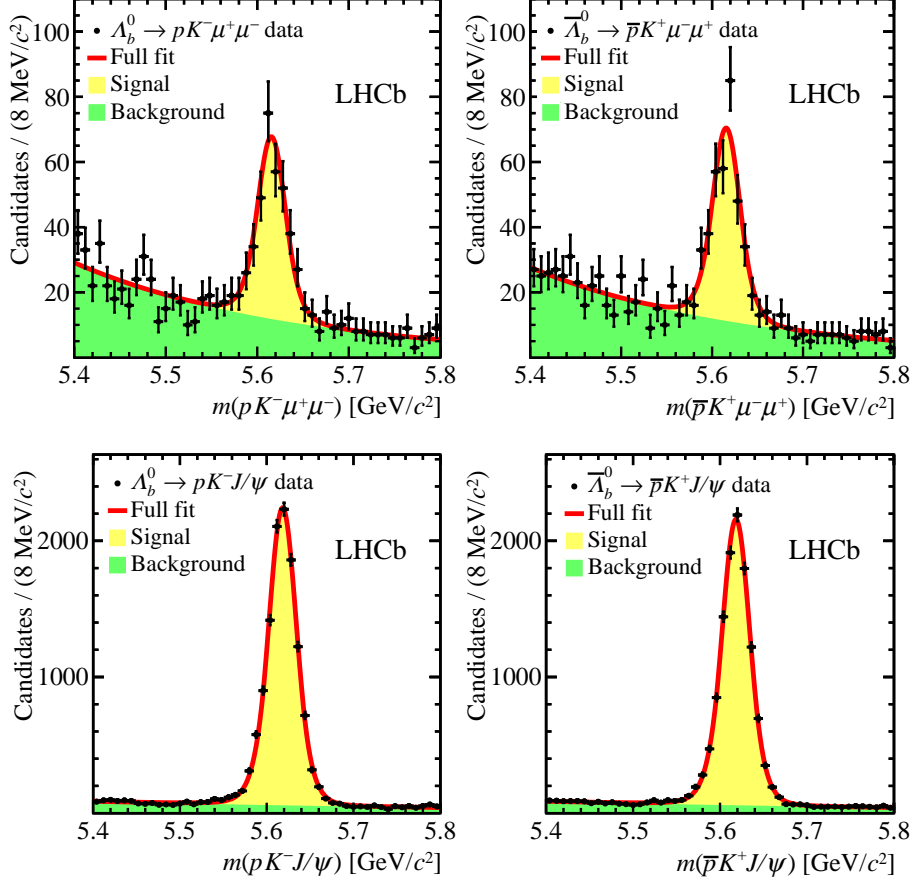


Figure 3: Invariant mass distributions of (top) $\Lambda_b^0 \rightarrow pK^- \mu^+ \mu^-$ and (bottom) $\Lambda_b^0 \rightarrow pK^- J/\psi$ candidates, with fit results superimposed. Plots refer to the (left) Λ_b^0 and (right) $\bar{\Lambda}_b^0$ subsamples.

within their uncertainties. This amounts to $\pm 0.10 \times 10^{-2}$ for the $\Delta\mathcal{A}_{CP}$ observable and to $\pm 0.02 \times 10^{-2}$ for $a_{CP}^{\hat{T}\text{-odd}}$ and $a_P^{\hat{T}\text{-odd}}$.

The above effects are the dominant sources of systematic uncertainties. Other possible sources of systematic uncertainties are considered. The experimental resolution on $C_{\hat{T}}$ is studied with simulated signal events. The effect of the fit model choice is studied by fitting simulated pseudoexperiments with an alternative fit model, in which the Crystal Ball functions are replaced with bifurcated Gaussian functions and the exponential background shape is replaced with a polynomial. Systematic effects from Λ_b^0 polarisation [34], multiple candidates, and residual physical backgrounds are also studied. These contributions have negligible impact on the measured asymmetries.

7 Conclusions

The first search for CP violation in the process $\Lambda_b^0 \rightarrow pK^- \mu^+ \mu^-$ is performed with a data sample containing 600 ± 44 signal decays, this representing the first observation of this Λ_b^0 decay mode. Two different CP -violating observables that are sensitive to different manifestations of CP violation, $\Delta\mathcal{A}_{CP}$ and $a_{CP}^{\hat{T}\text{-odd}}$, are measured. The parity-violating

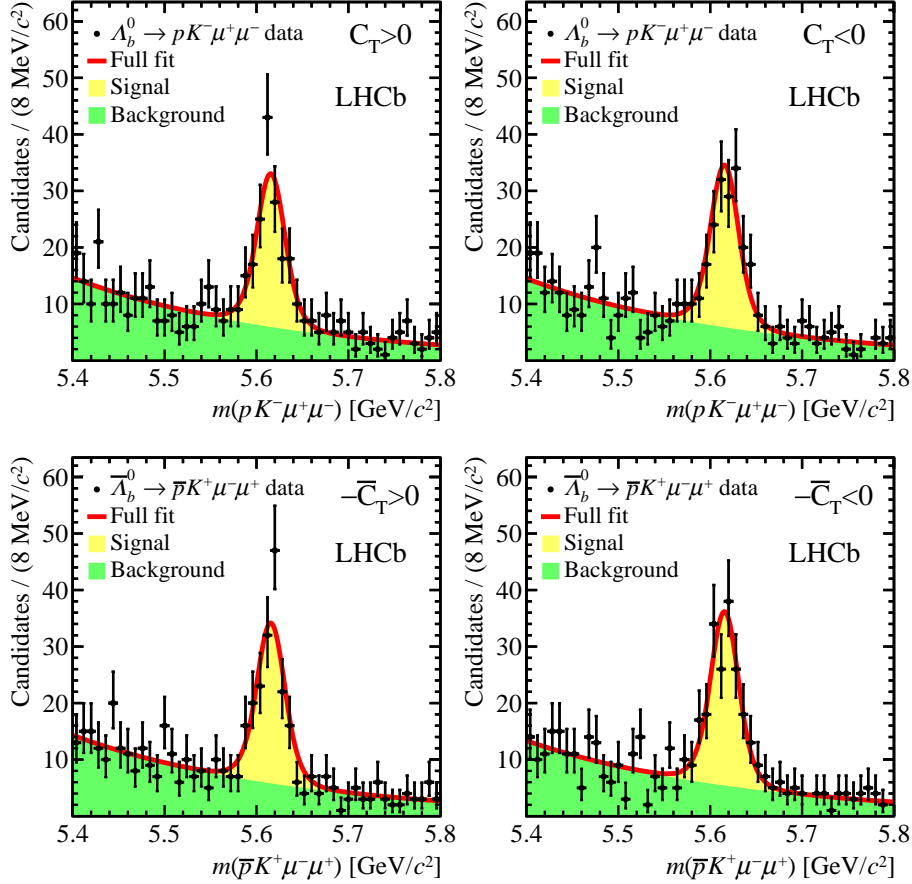


Figure 4: Invariant mass distributions of the $\Lambda_b^0 \rightarrow pK^-\mu^+\mu^-$ subsamples used for the $A_{\hat{T}}$ and $\bar{A}_{\hat{T}}$ measurements. Plots refer to (top) Λ_b^0 and (bottom) $\bar{\Lambda}_b^0$ decays divided into the subsamples (left) $C_{\hat{T}} > 0$, $-\bar{C}_{\hat{T}} > 0$ and (right) $C_{\hat{T}} < 0$, $-\bar{C}_{\hat{T}} < 0$.

observable $a_P^{\hat{T}\text{-odd}}$ is also measured. The values obtained are

$$\Delta\mathcal{A}_{CP} = (-3.5 \pm 5.0 \text{ (stat)} \pm 0.2 \text{ (syst)}) \times 10^{-2},$$

$$a_{CP}^{\hat{T}\text{-odd}} = (1.2 \pm 5.0 \text{ (stat)} \pm 0.7 \text{ (syst)}) \times 10^{-2},$$

$$a_P^{\hat{T}\text{-odd}} = (-4.8 \pm 5.0 \text{ (stat)} \pm 0.7 \text{ (syst)}) \times 10^{-2}.$$

The results are compatible with CP and parity conservation and agree with SM predictions for CPV [15,16], and with experimental results [35,36] for decays mediated by $b \rightarrow s\mu^+\mu^-$ transitions in B^0 and B^+ meson decays.

Acknowledgements

We express our gratitude to our colleagues in the CERN accelerator departments for the excellent performance of the LHC. We thank the technical and administrative staff at the LHCb institutes. We acknowledge support from CERN and from the national agencies: CAPES, CNPq, FAPERJ and FINEP (Brazil); MOST and NSFC (China);

CNRS/IN2P3 (France); BMBF, DFG and MPG (Germany); INFN (Italy); FOM and NWO (The Netherlands); MNiSW and NCN (Poland); MEN/IFA (Romania); MinES and FASO (Russia); MinECo (Spain); SNSF and SER (Switzerland); NASU (Ukraine); STFC (United Kingdom); NSF (USA). We acknowledge the computing resources that are provided by CERN, IN2P3 (France), KIT and DESY (Germany), INFN (Italy), SURF (The Netherlands), PIC (Spain), GridPP (United Kingdom), RRCKI and Yandex LLC (Russia), CSCS (Switzerland), IFIN-HH (Romania), CBPF (Brazil), PL-GRID (Poland) and OSC (USA). We are indebted to the communities behind the multiple open source software packages on which we depend. Individual groups or members have received support from AvH Foundation (Germany), EPLANET, Marie Skłodowska-Curie Actions and ERC (European Union), Conseil Général de Haute-Savoie, Labex ENIGMASS and OCEVU, Région Auvergne (France), RFBR and Yandex LLC (Russia), GVA, XuntaGal and GENCAT (Spain), Herchel Smith Fund, The Royal Society, Royal Commission for the Exhibition of 1851 and the Leverhulme Trust (United Kingdom).

References

- [1] J. H. Christenson, J. W. Cronin, V. L. Fitch, and R. Turlay, *Evidence for the 2π decay of the K_2^0 meson*, Phys. Rev. Lett. **13** (1964) 138.
- [2] N. Cabibbo, *Unitary symmetry and leptonic decays*, Phys. Rev. Lett. **10** (1963) 531.
- [3] M. Kobayashi and T. Maskawa, *CP Violation in the renormalizable theory of weak interaction*, Prog. Theo. Phys. **49** (1973) 652.
- [4] A. D. Sakharov, *Violation of CP invariance, C asymmetry, and baryon asymmetry of the universe*, Soviet Physics Uspekhi **34** (1991) 392.
- [5] M. B. Gavela, P. Hernandez, J. Orloff, and O. Pene, *Standard Model CP violation and baryon asymmetry*, Mod. Phys. Lett. **A9** (1994) 795, arXiv:hep-ph/9312215.
- [6] M. B. Gavela *et al.*, *Standard Model CP violation and baryon asymmetry. Part 2: Finite temperature*, Nucl. Phys. **B430** (1994) 382, arXiv:hep-ph/9406289.
- [7] LHCb collaboration, R. Aaij *et al.*, *Probing matter-antimatter asymmetries in beauty baryon decays*, Nature Physics (2017) , arXiv:1609.05216.
- [8] LHCb collaboration, A. A. Alves Jr. *et al.*, *The LHCb detector at the LHC*, JINST **3** (2008) S08005.
- [9] LHCb collaboration, R. Aaij *et al.*, *Measurement of b-hadron production fractions in 7 TeV pp collisions*, Phys. Rev. **D85** (2012) 032008, arXiv:1111.2357.
- [10] LHCb collaboration, R. Aaij *et al.*, *Observation of the $\Lambda_b^0 \rightarrow J/\psi p\pi^-$ decay*, JHEP **07** (2014) 103, arXiv:1406.0755.
- [11] LHCb collaboration, R. Aaij *et al.*, *Searches for Λ_b^0 and Ξ_b^0 decays to $K_S^0 p\pi^-$ and $K_S^0 pK^-$ final states with first observation of the $\Lambda_b^0 \rightarrow K_S^0 p\pi^-$ decay*, JHEP **04** (2014) 087, arXiv:1402.0770.
- [12] LHCb collaboration, R. Aaij *et al.*, *Observation of the $\Lambda_b^0 \rightarrow \Lambda\phi$ decay*, Phys. Lett. **B759** (2016) 282, arXiv:1603.02870.
- [13] LHCb collaboration, R. Aaij *et al.*, *Observations of $\Lambda_b^0 \rightarrow \Lambda K^+\pi^-$ and $\Lambda_b^0 \rightarrow \Lambda K^+K^-$ decays and searches for other Λ_b^0 and Ξ_b^0 decays to Λh^+h^- final states*, JHEP **05** (2016) 081, arXiv:1603.00413.
- [14] R. Gauld, F. Goertz, and U. Haisch, *An explicit Z' -boson explanation of the $B \rightarrow K^*\mu^+\mu^-$ anomaly*, JHEP **01** (2014) 069, arXiv:1310.1082.
- [15] M. A. Paracha, I. Ahmed, and M. J. Aslam, *Imprints of CP violation asymmetries in rare $\Lambda_b \rightarrow \Lambda\ell^+\ell^-$ decay in family non-universal Z' model*, PTEP **2015** (2015) 033B04, arXiv:1408.4318.
- [16] A. K. Alok *et al.*, *New physics in $b \rightarrow s\mu^+\mu^-$: CP-violating observables*, JHEP **11** (2011) 122, arXiv:1103.5344.

- [17] G. Durieux and Y. Grossman, *Probing CP violation systematically in differential distributions*, Phys. Rev. **D92** (2015) 076013, arXiv:1508.03054.
- [18] M. Gronau and J. L. Rosner, *Triple product asymmetries in K , $D_{(s)}$ and $B_{(s)}$ decays*, Phys. Rev. **D84** (2011) 096013, arXiv:1107.1232.
- [19] LHCb collaboration, R. Aaij *et al.*, *LHCb detector performance*, Int. J. Mod. Phys. **A30** (2015) 1530022, arXiv:1412.6352.
- [20] R. Aaij *et al.*, *The LHCb trigger and its performance in 2011*, JINST **8** (2013) P04022, arXiv:1211.3055.
- [21] T. Sjöstrand, S. Mrenna, and P. Skands, *PYTHIA 6.4 physics and manual*, JHEP **05** (2006) 026, arXiv:hep-ph/0603175.
- [22] T. Sjöstrand, S. Mrenna, and P. Skands, *A brief introduction to PYTHIA 8.1*, Comput. Phys. Commun. **178** (2008) 852, arXiv:0710.3820.
- [23] I. Belyaev *et al.*, *Handling of the generation of primary events in Gauss, the LHCb simulation framework*, J. Phys. Conf. Ser. **331** (2011) 032047.
- [24] D. J. Lange, *The EvtGen particle decay simulation package*, Nucl. Instrum. Meth. **A462** (2001) 152.
- [25] P. Golonka and Z. Was, *PHOTOS Monte Carlo: A precision tool for QED corrections in Z and W decays*, Eur. Phys. J. **C45** (2006) 97, arXiv:hep-ph/0506026.
- [26] Geant4 collaboration, J. Allison *et al.*, *Geant4 developments and applications*, IEEE Trans. Nucl. Sci. **53** (2006) 270.
- [27] M. Clemencic *et al.*, *The LHCb simulation application, Gauss: Design, evolution and experience*, J. Phys. Conf. Ser. **331** (2011) 032023.
- [28] L. Breiman, J. H. Friedman, R. A. Olshen, and C. J. Stone, *Classification and regression trees*, Wadsworth international group, Belmont, California, USA, 1984.
- [29] B. P. Roe *et al.*, *Boosted decision trees as an alternative to artificial neural networks for particle identification*, Nucl. Instrum. Meth. **A543** (2005) 577, arXiv:physics/0408124.
- [30] Y. Freund and R. E. Schapire, *A decision-theoretic generalization of on-line learning and an application to boosting*, J. Comput. Syst. Sci. **55** (1997) 119.
- [31] LHCb collaboration, R. Aaij *et al.*, *Search for the rare decays $B_s^0 \rightarrow \mu^+\mu^-$ and $B^0 \rightarrow \mu^+\mu^-$* , Phys. Lett. **B699** (2011) 330, arXiv:1103.2465.
- [32] LHCb collaboration, R. Aaij *et al.*, *Determination of the quark coupling strength $|V_{ub}|$ using baryonic decays*, Nature Phys. **11** (2015) 743, arXiv:1504.01568.
- [33] T. Skwarnicki, *A study of the radiative cascade transitions between the Upsilon-prime and Upsilon resonances*, PhD thesis, Institute of Nuclear Physics, Krakow, 1986, DESY-F31-86-02.

- [34] LHCb collaboration, R. Aaij *et al.*, *Measurements of the $\Lambda_b^0 \rightarrow J/\psi \Lambda$ decay amplitudes and the Λ_b^0 polarisation in pp collisions at $\sqrt{s} = 7$ TeV*, Phys. Lett. **B724** (2013) 27, [arXiv:1302.5578](#).
- [35] LHCb collaboration, R. Aaij *et al.*, *Measurement of CP asymmetries in the decays $B^0 \rightarrow K^{*0} \mu^+ \mu^-$ and $B^+ \rightarrow K^+ \mu^+ \mu^-$* , JHEP **09** (2014) 177, [arXiv:1408.0978](#).
- [36] BaBar collaboration, J. P. Lees *et al.*, *Measurement of branching fractions and rate asymmetries in the rare decays $B \rightarrow K^{(*)} l^+ l^-$* , Phys. Rev. **D86** (2012) 032012, [arXiv:1204.3933](#).

LHCb collaboration

R. Aaij⁴⁰, B. Adeva³⁹, M. Adinolfi⁴⁸, Z. Ajaltouni⁵, S. Akar⁵⁹, J. Albrecht¹⁰, F. Alessio⁴⁰, M. Alexander⁵³, S. Ali⁴³, G. Alkhazov³¹, P. Alvarez Cartelle⁵⁵, A.A. Alves Jr⁵⁹, S. Amato², S. Amerio²³, Y. Amhis⁷, L. An³, L. Anderlini¹⁸, G. Andreassi⁴¹, M. Andreotti^{17,g}, J.E. Andrews⁶⁰, R.B. Appleby⁵⁶, F. Archilli⁴³, P. d'Argent¹², J. Arnau Romeu⁶, A. Artamonov³⁷, M. Artuso⁶¹, E. Aslanides⁶, G. Auriemma²⁶, M. Baalouch⁵, I. Babuschkin⁵⁶, S. Bachmann¹², J.J. Back⁵⁰, A. Badalov³⁸, C. Baesso⁶², S. Baker⁵⁵, V. Balagura^{7,c}, W. Baldini¹⁷, R.J. Barlow⁵⁶, C. Barschel⁴⁰, S. Barsuk⁷, W. Barter⁵⁶, F. Baryshnikov³², M. Baszczyk^{27,l}, V. Batozskaya²⁹, B. Batsukh⁶¹, V. Battista⁴¹, A. Bay⁴¹, L. Beaucourt⁴, J. Beddow⁵³, F. Bedeschi²⁴, I. Bediaga¹, L.J. Bel⁴³, V. Bellee⁴¹, N. Belloli^{21,i}, K. Belous³⁷, I. Belyaev³², E. Ben-Haim⁸, G. Bencivenni¹⁹, S. Benson⁴³, A. Berezhnoy³³, R. Bernet⁴², A. Bertolin²³, C. Betancourt⁴², F. Betti¹⁵, M.-O. Bettler⁴⁰, M. van Beuzekom⁴³, I.a. Bezshyiko⁴², S. Bifani⁴⁷, P. Billoir⁸, T. Bird⁵⁶, A. Birnkraut¹⁰, A. Bitadze⁵⁶, A. Bizzeti^{18,u}, T. Blake⁵⁰, F. Blanc⁴¹, J. Blouw^{11,†}, S. Blusk⁶¹, V. Bocci²⁶, T. Boettcher⁵⁸, A. Bondar^{36,w}, N. Bondar^{31,40}, W. Bonivento¹⁶, I. Bordyuzhin³², A. Borgheresi^{21,i}, S. Borghi⁵⁶, M. Borisyak³⁵, M. Borsato³⁹, F. Bossu⁷, M. Boubdir⁹, T.J.V. Bowcock⁵⁴, E. Bowen⁴², C. Bozzi^{17,40}, S. Braun¹², M. Britsch¹², T. Britton⁶¹, J. Brodzicka⁵⁶, E. Buchanan⁴⁸, C. Burr⁵⁶, A. Bursche², J. Buytaert⁴⁰, S. Cadeddu¹⁶, R. Calabrese^{17,g}, M. Calvi^{21,i}, M. Calvo Gomez^{38,m}, A. Camboni³⁸, P. Campana¹⁹, D.H. Campora Perez⁴⁰, L. Capriotti⁵⁶, A. Carbone^{15,e}, G. Carboni^{25,j}, R. Cardinale^{20,h}, A. Cardini¹⁶, P. Carniti^{21,i}, L. Carson⁵², K. Carvalho Akiba², G. Casse⁵⁴, L. Cassina^{21,i}, L. Castillo Garcia⁴¹, M. Cattaneo⁴⁰, G. Cavallero²⁰, R. Cenci^{24,t}, D. Chamont⁷, M. Charles⁸, Ph. Charpentier⁴⁰, G. Chatzikonstantinidis⁴⁷, M. Chefdeville⁴, S. Chen⁵⁶, S.F. Cheung⁵⁷, V. Chobanova³⁹, M. Chrzaszcz^{42,27}, X. Cid Vidal³⁹, G. Ciezarek⁴³, P.E.L. Clarke⁵², M. Clemencic⁴⁰, H.V. Cliff⁴⁹, J. Closier⁴⁰, V. Coco⁵⁹, J. Cogan⁶, E. Cogneras⁵, V. Cogoni^{16,40,f}, L. Cojocariu³⁰, P. Collins⁴⁰, A. Comerma-Montells¹², A. Contu⁴⁰, A. Cook⁴⁸, G. Coombs⁴⁰, S. Coquereau³⁸, G. Corti⁴⁰, M. Corvo^{17,g}, C.M. Costa Sobral⁵⁰, B. Couturier⁴⁰, G.A. Cowan⁵², D.C. Craik⁵², A. Crocombe⁵⁰, M. Cruz Torres⁶², S. Cunliffe⁵⁵, R. Currie⁵⁵, C. D'Ambrosio⁴⁰, F. Da Cunha Marinho², E. Dall'Occo⁴³, J. Dalseno⁴⁸, P.N.Y. David⁴³, A. Davis³, K. De Bruyn⁶, S. De Capua⁵⁶, M. De Cian¹², J.M. De Miranda¹, L. De Paula², M. De Serio^{14,d}, P. De Simone¹⁹, C.T. Dean⁵³, D. Decamp⁴, M. Deckenhoff¹⁰, L. Del Buono⁸, M. Demmer¹⁰, A. Dendek²⁸, D. Derkach³⁵, O. Deschamps⁵, F. Dettori⁴⁰, B. Dey²², A. Di Canto⁴⁰, H. Dijkstra⁴⁰, F. Dordei⁴⁰, M. Dorigo⁴¹, A. Dosil Suárez³⁹, A. Dovbnya⁴⁵, K. Dreimanis⁵⁴, L. Dufour⁴³, G. Dujany⁵⁶, K. Dungs⁴⁰, P. Durante⁴⁰, R. Dzhelyadin³⁷, A. Dziurda⁴⁰, A. Dzyuba³¹, N. Déléage⁴, S. Easo⁵¹, M. Ebert⁵², U. Egede⁵⁵, V. Egorychev³², S. Eidelman^{36,w}, S. Eisenhardt⁵², U. Eitschberger¹⁰, R. Ekelhof¹⁰, L. Eklund⁵³, S. Ely⁶¹, S. Esen¹², H.M. Evans⁴⁹, T. Evans⁵⁷, A. Falabella¹⁵, N. Farley⁴⁷, S. Farry⁵⁴, R. Fay⁵⁴, D. Fazzini^{21,i}, D. Ferguson⁵², A. Fernandez Prieto³⁹, F. Ferrari^{15,40}, F. Ferreira Rodrigues², M. Ferro-Luzzi⁴⁰, S. Filippov³⁴, R.A. Fini¹⁴, M. Fiore^{17,g}, M. Fiorini^{17,g}, M. Firlej²⁸, C. Fitzpatrick⁴¹, T. Fiutowski²⁸, F. Fleuret^{7,b}, K. Fohl⁴⁰, M. Fontana^{16,40}, F. Fontanelli^{20,h}, D.C. Forshaw⁶¹, R. Forty⁴⁰, V. Franco Lima⁵⁴, M. Frank⁴⁰, C. Frei⁴⁰, J. Fu^{22,q}, W. Funk⁴⁰, E. Furfaro^{25,j}, C. Färber⁴⁰, A. Gallas Torreira³⁹, D. Galli^{15,e}, S. Gallorini²³, S. Gambetta⁵², M. Gandelman², P. Gandini⁵⁷, Y. Gao³, L.M. Garcia Martin⁶⁹, J. García Pardiñas³⁹, J. Garra Tico⁴⁹, L. Garrido³⁸, P.J. Garsed⁴⁹, D. Gascon³⁸, C. Gaspar⁴⁰, L. Gavardi¹⁰, G. Gazzoni⁵, D. Gerick¹², E. Gersabeck¹², M. Gersabeck⁵⁶, T. Gershon⁵⁰, Ph. Ghez⁴, S. Gianì⁴¹, V. Gibson⁴⁹, O.G. Girard⁴¹, L. Giubega³⁰, K. Gizdov⁵², V.V. Gligorov⁸, D. Golubkov³², A. Golutvin^{55,40}, A. Gomes^{1,a}, I.V. Gorelov³³, C. Gotti^{21,i}, R. Graciani Diaz³⁸, L.A. Granado Cardoso⁴⁰, E. Graugés³⁸, E. Graverini⁴², G. Graziani¹⁸, A. Greco³⁰, P. Griffith¹⁶, L. Grillo^{21,40,i}, B.R. Gruberg Cazon⁵⁷, O. Grünberg⁶⁷, E. Gushchin³⁴, Yu. Guz³⁷, T. Gys⁴⁰, C. Göbel⁶², T. Hadavizadeh⁵⁷, C. Hadjivasiliou⁵, G. Haefeli⁴¹, C. Haen⁴⁰, S.C. Haines⁴⁹,

B. Hamilton⁶⁰, X. Han¹², S. Hansmann-Menzemer¹², N. Harnew⁵⁷, S.T. Harnew⁴⁸,
 J. Harrison⁵⁶, M. Hatch⁴⁰, J. He⁶³, T. Head⁴¹, A. Heister⁹, K. Hennessy⁵⁴, P. Henrard⁵,
 L. Henry⁸, E. van Herwijnen⁴⁰, M. Heß⁶⁷, A. Hicheur², D. Hill⁵⁷, C. Hombach⁵⁶,
 P.H. Hopchev⁴¹, W. Hulsbergen⁴³, T. Humair⁵⁵, M. Hushchyn³⁵, D. Hutchcroft⁵⁴, M. Idzik²⁸,
 P. Ilten⁵⁸, R. Jacobsson⁴⁰, A. Jaeger¹², J. Jalocha⁵⁷, E. Jans⁴³, A. Jawahery⁶⁰, F. Jiang³,
 M. John⁵⁷, D. Johnson⁴⁰, C.R. Jones⁴⁹, C. Joram⁴⁰, B. Jost⁴⁰, N. Jurik⁵⁷, S. Kandybei⁴⁵,
 M. Karacson⁴⁰, J.M. Kariuki⁴⁸, S. Karodia⁵³, M. Kecke¹², M. Kelsey⁶¹, M. Kenzie⁴⁹, T. Ketel⁴⁴,
 E. Khairullin³⁵, B. Khanji¹², C. Khurewathanakul⁴¹, T. Kirn⁹, S. Klaver⁵⁶, K. Klimaszewski²⁹,
 S. Koliiev⁴⁶, M. Kolpin¹², I. Komarov⁴¹, R.F. Koopman⁴⁴, P. Koppenburg⁴³, A. Kosmyntseva³²,
 A. Kozachuk³³, M. Kozeiha⁵, L. Kravchuk³⁴, K. Kreplin¹², M. Kreps⁵⁰, P. Krokovny^{36,w},
 F. Kruse¹⁰, W. Krzemien²⁹, W. Kucewicz^{27,l}, M. Kucharczyk²⁷, V. Kudryavtsev^{36,w},
 A.K. Kuonen⁴¹, K. Kurek²⁹, T. Kvaratskheliya^{32,40}, D. Lacarrere⁴⁰, G. Lafferty⁵⁶, A. Lai¹⁶,
 G. Lanfranchi¹⁹, C. Langenbruch⁹, T. Latham⁵⁰, C. Lazzeroni⁴⁷, R. Le Gac⁶, J. van Leerdam⁴³,
 A. Leflat^{33,40}, J. Lefrançois⁷, R. Lefèvre⁵, F. Lemaitre⁴⁰, E. Lemos Cid³⁹, O. Leroy⁶,
 T. Lesiak²⁷, B. Leverington¹², T. Li³, Y. Li⁷, T. Likhomanenko^{35,68}, R. Lindner⁴⁰, C. Linn⁴⁰,
 F. Lionetto⁴², X. Liu³, D. Loh⁵⁰, I. Longstaff⁵³, J.H. Lopes², D. Lucchesi^{23,o},
 M. Lucio Martinez³⁹, H. Luo⁵², A. Lupato²³, E. Luppi^{17,g}, O. Lupton⁴⁰, A. Lusiani²⁴, X. Lyu⁶³,
 F. Machefert⁷, F. Maciuc³⁰, O. Maev³¹, K. Maguire⁵⁶, S. Malde⁵⁷, A. Malinin⁶⁸, T. Maltsev³⁶,
 G. Manca^{16,f}, G. Mancinelli⁶, P. Manning⁶¹, D. Marangotto^{22,q}, J. Maratas^{5,v}, J.F. Marchand⁴,
 U. Marconi¹⁵, C. Marin Benito³⁸, M. Marinangeli⁴¹, P. Marino^{24,t}, J. Marks¹², G. Martellotti²⁶,
 M. Martin⁶, M. Martinelli⁴¹, D. Martinez Santos³⁹, F. Martinez Vidal⁶⁹, D. Martins Tostes²,
 L.M. Massacrier⁷, A. Massafferri¹, R. Matev⁴⁰, A. Mathad⁵⁰, Z. Mathe⁴⁰, C. Matteuzzi²¹,
 A. Mauri⁴², E. Maurice^{7,b}, B. Maurin⁴¹, A. Mazurov⁴⁷, M. McCann^{55,40}, A. McNab⁵⁶,
 R. McNulty¹³, B. Meadows⁵⁹, F. Meier¹⁰, M. Meissner¹², D. Melnychuk²⁹, M. Merk⁴³,
 A. Merli^{22,q}, E. Michielin²³, D.A. Milanes⁶⁶, M.-N. Minard⁴, D.S. Mitzel¹², A. Mogini⁸,
 J. Molina Rodriguez¹, I.A. Monroy⁶⁶, S. Monteil⁵, M. Morandin²³, P. Morawski²⁸, A. Mordà⁶,
 M.J. Morello^{24,t}, O. Morgunova⁶⁸, J. Moron²⁸, A.B. Morris⁵², R. Mountain⁶¹, F. Muheim⁵²,
 M. Mulder⁴³, M. Mussini¹⁵, D. Müller⁵⁶, J. Müller¹⁰, K. Müller⁴², V. Müller¹⁰, P. Naik⁴⁸,
 T. Nakada⁴¹, R. Nandakumar⁵¹, A. Nandi⁵⁷, I. Nasteva², M. Needham⁵², N. Neri²²,
 S. Neubert¹², N. Neufeld⁴⁰, M. Neuner¹², T.D. Nguyen⁴¹, C. Nguyen-Mau^{41,n}, S. Nieswand⁹,
 R. Niet¹⁰, N. Nikitin³³, T. Nikodem¹², A. Nogay⁶⁸, A. Novoselov³⁷, D.P. O’Hanlon⁵⁰,
 A. Oblakowska-Mucha²⁸, V. Obraztsov³⁷, S. Ogilvy¹⁹, R. Oldeman^{16,f}, C.J.G. Onderwater⁷⁰,
 J.M. Otalora Goicochea², A. Otto⁴⁰, P. Owen⁴², A. Oyanguren⁶⁹, P.R. Pais⁴¹, A. Palano^{14,d},
 M. Palutan¹⁹, A. Papanestis⁵¹, M. Pappagallo^{14,d}, L.L. Pappalardo^{17,g}, W. Parker⁶⁰,
 C. Parkes⁵⁶, G. Passaleva¹⁸, A. Pastore^{14,d}, G.D. Patel⁵⁴, M. Patel⁵⁵, C. Patrignani^{15,e},
 A. Pearce⁴⁰, A. Pellegrino⁴³, G. Penso²⁶, M. Pepe Altarelli⁴⁰, S. Perazzini⁴⁰, P. Perret⁵,
 L. Pescatore⁴¹, K. Petridis⁴⁸, A. Petrolini^{20,h}, A. Petrov⁶⁸, M. Petruzzo^{22,q},
 E. Picatoste Olloqui³⁸, B. Pietrzyk⁴, M. Pikiés²⁷, D. Pinci²⁶, A. Pistone²⁰, A. Piucci¹²,
 V. Placinta³⁰, S. Playfer⁵², M. Plo Casasus³⁹, T. Poikela⁴⁰, F. Polci⁸, A. Poluektov^{50,36},
 I. Polyakov⁶¹, E. Polcarpo², G.J. Pomery⁴⁸, A. Popov³⁷, D. Popov^{11,40}, B. Popovici³⁰,
 S. Poslavskii³⁷, C. Potterat², E. Price⁴⁸, J.D. Price⁵⁴, J. Prisciandaro^{39,40}, A. Pritchard⁵⁴,
 C. Prouve⁴⁸, V. Pugatch⁴⁶, A. Puig Navarro⁴², G. Punzi^{24,p}, W. Qian⁵⁰, R. Quagliani^{7,48},
 B. Rachwal²⁷, J.H. Rademacker⁴⁸, M. Rama²⁴, M. Ramos Pernas³⁹, M.S. Rangel², I. Raniuk^{45,†},
 F. Ratnikov³⁵, G. Raven⁴⁴, F. Redi⁵⁵, S. Reichert¹⁰, A.C. dos Reis¹, C. Remon Alepuz⁶⁹,
 V. Renaudin⁷, S. Ricciardi⁵¹, S. Richards⁴⁸, M. Rihl⁴⁰, K. Rinnert⁵⁴, V. Rives Molina³⁸,
 P. Robbe^{7,40}, A.B. Rodrigues¹, E. Rodrigues⁵⁹, J.A. Rodriguez Lopez⁶⁶, P. Rodriguez Perez^{56,†},
 A. Rogozhnikov³⁵, S. Roiser⁴⁰, A. Rollings⁵⁷, V. Romanovskiy³⁷, A. Romero Vidal³⁹,
 J.W. Ronayne¹³, M. Rotondo¹⁹, M.S. Rudolph⁶¹, T. Ruf⁴⁰, P. Ruiz Valls⁶⁹,
 J.J. Saborido Silva³⁹, E. Sadykhov³², N. Sagidova³¹, B. Saitta^{16,f}, V. Salustino Guimaraes¹,
 C. Sanchez Mayordomo⁶⁹, B. Sanmartin Sedes³⁹, R. Santacesaria²⁶, C. Santamarina Rios³⁹,

M. Santimaria¹⁹, E. Santovetti^{25,j}, A. Sarti^{19,k}, C. Satriano^{26,s}, A. Satta²⁵, D.M. Saunders⁴⁸, D. Savrina^{32,33}, S. Schael⁹, M. Schellenberg¹⁰, M. Schiller⁵³, H. Schindler⁴⁰, M. Schlupp¹⁰, M. Schmelling¹¹, T. Schmelzer¹⁰, B. Schmidt⁴⁰, O. Schneider⁴¹, A. Schopper⁴⁰, K. Schubert¹⁰, M. Schubiger⁴¹, M.-H. Schune⁷, R. Schwemmer⁴⁰, B. Sciascia¹⁹, A. Sciubba^{26,k}, A. Semennikov³², A. Sergi⁴⁷, N. Serra⁴², J. Serrano⁶, L. Sestini²³, P. Seyfert²¹, M. Shapkin³⁷, I. Shapoval⁴⁵, Y. Shcheglov³¹, T. Shears⁵⁴, L. Shekhtman^{36,w}, V. Shevchenko⁶⁸, B.G. Siddi^{17,40}, R. Silva Coutinho⁴², L. Silva de Oliveira², G. Simi^{23,o}, S. Simone^{14,d}, M. Sirendi⁴⁹, N. Skidmore⁴⁸, T. Skwarnicki⁶¹, E. Smith⁵⁵, I.T. Smith⁵², J. Smith⁴⁹, M. Smith⁵⁵, H. Snoek⁴³, I. Soares Lavra¹, M.D. Sokoloff⁵⁹, F.J.P. Soler⁵³, B. Souza De Paula², B. Spaan¹⁰, P. Spradlin⁵³, S. Sridharan⁴⁰, F. Stagni⁴⁰, M. Stahl¹², S. Stahl⁴⁰, P. Stefko⁴¹, S. Stefkova⁵⁵, O. Steinkamp⁴², S. Stemmler¹², O. Stenyakin³⁷, H. Stevens¹⁰, S. Stevenson⁵⁷, S. Stoica³⁰, S. Stone⁶¹, B. Storaci⁴², S. Stracka^{24,p}, M. Straticiu³⁰, U. Straumann⁴², L. Sun⁶⁴, W. Sutcliffe⁵⁵, K. Swientek²⁸, V. Syropoulos⁴⁴, M. Szczekowski²⁹, T. Szumlak²⁸, S. T’Jampens⁴, A. Tayduganov⁶, T. Tekampe¹⁰, G. Tellarini^{17,g}, F. Teubert⁴⁰, E. Thomas⁴⁰, J. van Tilburg⁴³, M.J. Tilley⁵⁵, V. Tisserand⁴, M. Tobin⁴¹, S. Tolk⁴⁹, L. Tomassetti^{17,g}, D. Tonelli⁴⁰, S. Topp-Joergensen⁵⁷, F. Toriello⁶¹, E. Tournefier⁴, S. Tourneur⁴¹, K. Trabelsi⁴¹, M. Traill⁵³, M.T. Tran⁴¹, M. Tresch⁴², A. Trisovic⁴⁰, A. Tsaregorodtsev⁶, P. Tsopelas⁴³, A. Tully⁴⁹, N. Tuning⁴³, A. Ukleja²⁹, A. Ustyuzhanin³⁵, U. Uwer¹², C. Vacca^{16,f}, V. Vagnoni^{15,40}, A. Valassi⁴⁰, S. Valat⁴⁰, G. Valenti¹⁵, R. Vazquez Gomez¹⁹, P. Vazquez Regueiro³⁹, S. Vecchi¹⁷, M. van Veghel⁴³, J.J. Velthuis⁴⁸, M. Veltri^{18,r}, G. Veneziano⁵⁷, A. Venkateswaran⁶¹, M. Vernet⁵, M. Vesterinen¹², J.V. Viana Barbosa⁴⁰, B. Viaud⁷, D. Vieira⁶³, M. Vieites Diaz³⁹, H. Viemann⁶⁷, X. Vilasis-Cardona^{38,m}, M. Vitti⁴⁹, V. Volkov³³, A. Vollhardt⁴², B. Voneki⁴⁰, A. Vorobyev³¹, V. Vorobyev^{36,w}, C. Voß⁹, J.A. de Vries⁴³, C. Vázquez Sierra³⁹, R. Waldi⁶⁷, C. Wallace⁵⁰, R. Wallace¹³, J. Walsh²⁴, J. Wang⁶¹, D.R. Ward⁴⁹, H.M. Wark⁵⁴, N.K. Watson⁴⁷, D. Websdale⁵⁵, A. Weiden⁴², M. Whitehead⁴⁰, J. Wicht⁵⁰, G. Wilkinson^{57,40}, M. Wilkinson⁶¹, M. Williams⁴⁰, M.P. Williams⁴⁷, M. Williams⁵⁸, T. Williams⁴⁷, F.F. Wilson⁵¹, J. Wimberley⁶⁰, J. Wishahi¹⁰, W. Wislicki²⁹, M. Witek²⁷, G. Wormser⁷, S.A. Wotton⁴⁹, K. Wraight⁵³, K. Wyllie⁴⁰, Y. Xie⁶⁵, Z. Xing⁶¹, Z. Xu⁴, Z. Yang³, Y. Yao⁶¹, H. Yin⁶⁵, J. Yu⁶⁵, X. Yuan^{36,w}, O. Yushchenko³⁷, K.A. Zarebski⁴⁷, M. Zavertyaev^{11,c}, L. Zhang³, Y. Zhang⁷, A. Zhelezov¹², Y. Zheng⁶³, X. Zhu³, V. Zhukov³³, S. Zucchelli¹⁵.

¹Centro Brasileiro de Pesquisas Físicas (CBPF), Rio de Janeiro, Brazil

²Universidade Federal do Rio de Janeiro (UFRJ), Rio de Janeiro, Brazil

³Center for High Energy Physics, Tsinghua University, Beijing, China

⁴LAPP, Université Savoie Mont-Blanc, CNRS/IN2P3, Annecy-Le-Vieux, France

⁵Clermont Université, Université Blaise Pascal, CNRS/IN2P3, LPC, Clermont-Ferrand, France

⁶CPPM, Aix-Marseille Université, CNRS/IN2P3, Marseille, France

⁷LAL, Université Paris-Sud, CNRS/IN2P3, Orsay, France

⁸LPNHE, Université Pierre et Marie Curie, Université Paris Diderot, CNRS/IN2P3, Paris, France

⁹I. Physikalisches Institut, RWTH Aachen University, Aachen, Germany

¹⁰Fakultät Physik, Technische Universität Dortmund, Dortmund, Germany

¹¹Max-Planck-Institut für Kernphysik (MPIK), Heidelberg, Germany

¹²Physikalisches Institut, Ruprecht-Karls-Universität Heidelberg, Heidelberg, Germany

¹³School of Physics, University College Dublin, Dublin, Ireland

¹⁴Sezione INFN di Bari, Bari, Italy

¹⁵Sezione INFN di Bologna, Bologna, Italy

¹⁶Sezione INFN di Cagliari, Cagliari, Italy

¹⁷Sezione INFN di Ferrara, Ferrara, Italy

¹⁸Sezione INFN di Firenze, Firenze, Italy

¹⁹Laboratori Nazionali dell’INFN di Frascati, Frascati, Italy

²⁰Sezione INFN di Genova, Genova, Italy

²¹Sezione INFN di Milano Bicocca, Milano, Italy

²²Sezione INFN di Milano, Milano, Italy

- ²³ *Sezione INFN di Padova, Padova, Italy*
- ²⁴ *Sezione INFN di Pisa, Pisa, Italy*
- ²⁵ *Sezione INFN di Roma Tor Vergata, Roma, Italy*
- ²⁶ *Sezione INFN di Roma La Sapienza, Roma, Italy*
- ²⁷ *Henryk Niewodniczanski Institute of Nuclear Physics Polish Academy of Sciences, Kraków, Poland*
- ²⁸ *AGH - University of Science and Technology, Faculty of Physics and Applied Computer Science, Kraków, Poland*
- ²⁹ *National Center for Nuclear Research (NCBJ), Warsaw, Poland*
- ³⁰ *Horia Hulubei National Institute of Physics and Nuclear Engineering, Bucharest-Magurele, Romania*
- ³¹ *Petersburg Nuclear Physics Institute (PNPI), Gatchina, Russia*
- ³² *Institute of Theoretical and Experimental Physics (ITEP), Moscow, Russia*
- ³³ *Institute of Nuclear Physics, Moscow State University (SINP MSU), Moscow, Russia*
- ³⁴ *Institute for Nuclear Research of the Russian Academy of Sciences (INR RAN), Moscow, Russia*
- ³⁵ *Yandex School of Data Analysis, Moscow, Russia*
- ³⁶ *Budker Institute of Nuclear Physics (SB RAS), Novosibirsk, Russia*
- ³⁷ *Institute for High Energy Physics (IHEP), Protvino, Russia*
- ³⁸ *ICCUB, Universitat de Barcelona, Barcelona, Spain*
- ³⁹ *Universidad de Santiago de Compostela, Santiago de Compostela, Spain*
- ⁴⁰ *European Organization for Nuclear Research (CERN), Geneva, Switzerland*
- ⁴¹ *Institute of Physics, Ecole Polytechnique Fédérale de Lausanne (EPFL), Lausanne, Switzerland*
- ⁴² *Physik-Institut, Universität Zürich, Zürich, Switzerland*
- ⁴³ *Nikhef National Institute for Subatomic Physics, Amsterdam, The Netherlands*
- ⁴⁴ *Nikhef National Institute for Subatomic Physics and VU University Amsterdam, Amsterdam, The Netherlands*
- ⁴⁵ *NSC Kharkiv Institute of Physics and Technology (NSC KIPT), Kharkiv, Ukraine*
- ⁴⁶ *Institute for Nuclear Research of the National Academy of Sciences (KINR), Kyiv, Ukraine*
- ⁴⁷ *University of Birmingham, Birmingham, United Kingdom*
- ⁴⁸ *H.H. Wills Physics Laboratory, University of Bristol, Bristol, United Kingdom*
- ⁴⁹ *Cavendish Laboratory, University of Cambridge, Cambridge, United Kingdom*
- ⁵⁰ *Department of Physics, University of Warwick, Coventry, United Kingdom*
- ⁵¹ *STFC Rutherford Appleton Laboratory, Didcot, United Kingdom*
- ⁵² *School of Physics and Astronomy, University of Edinburgh, Edinburgh, United Kingdom*
- ⁵³ *School of Physics and Astronomy, University of Glasgow, Glasgow, United Kingdom*
- ⁵⁴ *Oliver Lodge Laboratory, University of Liverpool, Liverpool, United Kingdom*
- ⁵⁵ *Imperial College London, London, United Kingdom*
- ⁵⁶ *School of Physics and Astronomy, University of Manchester, Manchester, United Kingdom*
- ⁵⁷ *Department of Physics, University of Oxford, Oxford, United Kingdom*
- ⁵⁸ *Massachusetts Institute of Technology, Cambridge, MA, United States*
- ⁵⁹ *University of Cincinnati, Cincinnati, OH, United States*
- ⁶⁰ *University of Maryland, College Park, MD, United States*
- ⁶¹ *Syracuse University, Syracuse, NY, United States*
- ⁶² *Pontifícia Universidade Católica do Rio de Janeiro (PUC-Rio), Rio de Janeiro, Brazil, associated to ²*
- ⁶³ *University of Chinese Academy of Sciences, Beijing, China, associated to ³*
- ⁶⁴ *School of Physics and Technology, Wuhan University, Wuhan, China, associated to ³*
- ⁶⁵ *Institute of Particle Physics, Central China Normal University, Wuhan, Hubei, China, associated to ³*
- ⁶⁶ *Departamento de Física, Universidad Nacional de Colombia, Bogota, Colombia, associated to ⁸*
- ⁶⁷ *Institut für Physik, Universität Rostock, Rostock, Germany, associated to ¹²*
- ⁶⁸ *National Research Centre Kurchatov Institute, Moscow, Russia, associated to ³²*
- ⁶⁹ *Instituto de Física Corpuscular, Centro Mixto Universidad de Valencia - CSIC, Valencia, Spain, associated to ³⁸*
- ⁷⁰ *Van Swinderen Institute, University of Groningen, Groningen, The Netherlands, associated to ⁴³*

^a *Universidade Federal do Triângulo Mineiro (UFMT), Uberaba-MG, Brazil*

^b *Laboratoire Leprince-Ringuet, Palaiseau, France*

^c *P.N. Lebedev Physical Institute, Russian Academy of Science (LPI RAS), Moscow, Russia*

^d *Università di Bari, Bari, Italy*

^e *Università di Bologna, Bologna, Italy*

^f *Università di Cagliari, Cagliari, Italy*

^g *Università di Ferrara, Ferrara, Italy*

^h *Università di Genova, Genova, Italy*

ⁱ *Università di Milano Bicocca, Milano, Italy*

^j *Università di Roma Tor Vergata, Roma, Italy*

^k *Università di Roma La Sapienza, Roma, Italy*

^l *AGH - University of Science and Technology, Faculty of Computer Science, Electronics and Telecommunications, Kraków, Poland*

^m *LIFAEELS, La Salle, Universitat Ramon Llull, Barcelona, Spain*

ⁿ *Hanoi University of Science, Hanoi, Viet Nam*

^o *Università di Padova, Padova, Italy*

^p *Università di Pisa, Pisa, Italy*

^q *Università degli Studi di Milano, Milano, Italy*

^r *Università di Urbino, Urbino, Italy*

^s *Università della Basilicata, Potenza, Italy*

^t *Scuola Normale Superiore, Pisa, Italy*

^u *Università di Modena e Reggio Emilia, Modena, Italy*

^v *Iligan Institute of Technology (IIT), Iligan, Philippines*

^w *Novosibirsk State University, Novosibirsk, Russia*

[†] *Deceased*